Network View of Binary Cellular Automata

Yoshihiko Kayama

Department of Media and Information, BAIKA Women's University
2-19-5 Shukuno-sho, Ibaraki 567-8578, Osaka, Japan
y_kayama@ieee.org

Abstract. The network view of cellular automata focuses on the effective relationships between cells rather than the states themselves. In this article, we review a network representation presented in previous papers and present network graphs derived from all independent rules of one-dimensional elementary cellular automata and totalistic five-neighbor cellular automata. Removal of the transient effects of initial configurations improves the visibility of the dynamical characteristics of each rule. Power-law distributions of lifetimes and sizes of avalanches caused by one-cell perturbations of an attractor are exhibited by the derived network of Rule 11 (or 52) of totalistic five-neighbor cellular automata.

Keywords: Cellular Automaton, Complex Network, Scale-free.

1 Introduction

Originally proposed by von Neumann [1], cellular automata (CA) have been studied and applied to investigate complex phenomena in various kinds of research fields. The parallelism of CA rules and their ability to form complex patterns can be characterized by four kinds of patterns called Wolfram's classes: homogeneous (class I), periodic (class II), chaotic (class III), and complex (class IV) [2]. In particular, Conway's Game of Life, or simply Life, can generate a wide range of interesting behaviors and simulate a universal computer [3,4]. Alternatively, complex networks have been studied extensively in the wake of papers by Watts and Strogatz on small-world networks [5] and by Barabási and Albert on scale-free networks [6]. The small-world or scale-free topologies can be identified ubiquitously in social relationships, biological and chemical systems, the Internet, etc. Complex systems composed of some fundamental elements frequently organize such complex networks. Motivated by this point of view, we proposed a method to derive a network from a binary CA rule, called a "network representation." The networks derived from elementary CA (ECA) and five-neighbor totalistic CA (5TCA) rules can visualize the dynamical characteristics of each rule and their network parameters show behaviors corresponding to Wolfram's classes [7,8]. The network representation of Life was discussed in the previous article [9]. Life is not only a member of class IV but also one of the simplest examples of *self-organized criticality* (SOC). Bak, Tang and Wiesenfeld [10] discovered that critical behavior can emerge spontaneously from simple local interactions

G.C. Sirakoulis and S. Bandini (Eds.): ACRI 2012, LNCS 7495, pp. 224–233, 2012.

without any fine tunings of variable parameters. As in the case of the sandpile model discussed by the above-mentioned authors, scale invariance is also exhibited by the distributions of the lifetimes and sizes of avalanches launched in Life's rest state [11]. Our network representation can visualize the underlying tension causing the avalanches and correspondingly exhibit a scale-free nature in its degree distributions.

In this article, we review our network representation of binary CA and present network graphs derived from all independent ECA and 5TCA rules. In contrast to the previous study [8], one-cell perturbations are applied after a sufficiently long initial time in order to remove the transient effects of initial configurations. The characteristic parameters of derived networks, namely efficiency and cluster coefficients (CCs), exhibit more obvious correspondence with Wolfram's classes than previously observed. The size of an avalanche catalyzed by the one-cell perturbation of a rest state, i.e., an attractor, is defined by the total changes in out-degrees during its lifetime [12]. The derived network of a class IV candidate, rule 11 (equivalent to rule 52) of 5TCA, exhibits power-law distributions of the lifetimes and sizes of the avalanches.

The next section reviews our network representation of binary CA. Section three consists of two parts: the first presents sample network graphs of all the independent rules of ECA and 5TCA, and the second introduces Life networks of typical patterns and a rest state. Section four reports the characteristic parameters of derived networks and the power-law distributions of the 5TCA rule.

2 Network Representation

Now we consider a regular 1D grid of cells, each characterized by binary states that are updated synchronously in discrete time steps according to a CA rule. Each cell has $2r + 1$ neighbors which consist of the cell itself and its r local neighbors on both sides, where r denotes the radius. The state of a cell at the next time step is determined from the current states of the neighboring cells:

$$x_i(t+1) = f_R(x_{i-r}(t), ..., x_i(t), ..., x_{i+r}(t)), \tag{1}$$

where $x_i(t)$ denotes the state of the cell i at time t, and f_R is the transition function of a rule R. The term *configuration* refers to an assignment of states to all cells for a given time step; a configuration is given by $\boldsymbol{x}(t) = \sum_{i=0}^{N-1} x_i(t)\boldsymbol{e}_i$, where $\boldsymbol{e}_i$ denotes the i-th unit vector: $\boldsymbol{e}_i = (0, \cdots, 0, \overset{i}{1}, 0, \cdots, 0)$, and N is the grid size. Thus, the time transition of configuration $\boldsymbol{x}(t)$ with some boundary conditions is given by $\boldsymbol{x}(t+1) = \boldsymbol{f}_R(\boldsymbol{x}(t))$, where $\boldsymbol{f}_R$ represents a mapping on the configuration space $\{\boldsymbol{x}\}_N$ induced from the rule function f_R. After t time steps, the configuration of cells obtained from an initial configuration $\boldsymbol{\varphi}$ is given by $\boldsymbol{x}(t, \boldsymbol{\varphi}) = \boldsymbol{f}_R^t(\boldsymbol{\varphi})$.

After t_0 time steps from the initial configuration, a perturbation is given to the configuration $\boldsymbol{\varphi}_0 \equiv \boldsymbol{x}(t_0, \boldsymbol{\varphi})$. The perturbation effect after t_I time steps can be written as

$$\Delta\boldsymbol{x}(t_I, \boldsymbol{\varphi}_0) \equiv \boldsymbol{f}_R^{t_I}(\boldsymbol{\varphi}_0 + \Delta\boldsymbol{\varphi}_0) + \boldsymbol{f}_R^{t_I}(\boldsymbol{\varphi}_0) \pmod 2. \tag{2}$$

If we denote $\Delta_i \boldsymbol{\varphi}_0$ as a one-cell perturbation of cell i, then $\Delta_i \boldsymbol{\varphi}_0 = \boldsymbol{e}_i$ in the binary case, and Eq. (2) leads to

$$\Delta_i \boldsymbol{x}(t_I, \boldsymbol{\varphi}_0) \equiv \Delta_i \boldsymbol{f}_R^{t_I}(\boldsymbol{\varphi}_0) = \boldsymbol{A}_R(t_I, \boldsymbol{\varphi}_0) \bullet \boldsymbol{e}_i, \tag{3}$$

where the product of the right-hand side is the inner product, and

$$\boldsymbol{A}_R(t_I, \boldsymbol{\varphi}_0) \equiv \sum_{i=0}^{N-1} \Delta_i \boldsymbol{f}_R^{t_I}(\boldsymbol{\varphi}_0) \boldsymbol{e}_i \tag{4}$$

has an $N \times N$ matrix representation. If $\mathcal{N} \equiv \{\boldsymbol{e}_i\}$ defines a set of nodes, then each component $(\Delta_i \boldsymbol{f}_R^{t_I}(\boldsymbol{\varphi}_0))_j$ defines a one-to-one mapping: $\mathcal{N} \to \mathcal{N}$. Therefore, we call $(\Delta_i \boldsymbol{f}_R^{t_I}(\boldsymbol{\varphi}_0))_j$ a *directed edge* from node i to node j. Then, $(\mathcal{N}, \mathcal{N}, \Delta_i \boldsymbol{f}_R^{t_I}(\boldsymbol{\varphi}_0))$ defines a directed graph connecting node i to other nodes. Taking all the graphs into consideration, we define a network representation of binary CA as $(\mathcal{N}, \mathcal{N}, \boldsymbol{A}_R(t_I, \boldsymbol{\varphi}_0))$, and a matrix representation of $\boldsymbol{A}_R(t_I, \boldsymbol{\varphi}_0)$ is the adjacency matrix $[\boldsymbol{A}_R]_{i,j} = (\Delta_i \boldsymbol{f}_R^{t_I}(\boldsymbol{\varphi}_0))_j$.

In CA, the network view focuses on the effective relationships between cells rather than their states. The directed graph $(\mathcal{N}, \mathcal{N}, \Delta_i \boldsymbol{f}_R^{t_I(}(\boldsymbol{\varphi}_0))$ illustrates the effective information flow from a one-cell perturbation of the cell i after t_I time steps. The symmetries of the network representation were discussed in the previous papers [7,8], in which we defined a transformation of a rule function called the *diminished-radix complement* $\hat{f}_R$ in addition to the mirror (left-right reflection), complement (0-1 exchange), and mirror-complement: $\hat{f}_R(x_{i-r}, ..., x_i, ..., x_{i+r}) \equiv f_R(\bar{x}_{i-r}, ..., \bar{x}_i, ..., \bar{x}_{i+r})$, where $\bar{x}$ is the complement of x. The transformation defines a new pairing of rules and if the two rules are self-complementary, their network representations are equivalent.

3 Sample Networks

– ECA and 5TCA rules

ECA are the simplest nontrivial CA with $r = 1$ and the $2^3 = 8$ different neighborhood configurations result in $2^8 = 256$ possible rules. Although five-neighbor ($r = 2$) CA contain 2^{32} rules, the totalistic CA (5TCA) are more restricted and contain $2^6 = 64$ rules. We follow a standard naming convention invented by Wolfram [2,13] that gives each rule in ECA and 5TCA a number from 0 to 255 and 0 to 63, respectively. To avoid confusion, we add the letter "T" to the Wolfram code of the 5TCA rules, e.g., rule $T52$. Taking all symmetries into consideration, we obtained the number of rules having non-trivial and independent networks as 73 in ECA and 26 in 5TCA [8]. The diminished-radix complement pairs of self-complement rules were also listed.

Sample networks of the independent rules are listed in the Appendix with $N = 41$ and $t_0 = 1000$. In order to ensure that each cell has causal relationships with all the other cells and to avoid repetitions, the time interval t_I was set to $[N/2]$ and $[N/4]$ for ECA and 5TCA, respectively, where [n] represents the maximum integer not exceeding n. The red and gray dots on the circumference of the graphs represent the active and inactive cells, respectively. Directed links are drawn with a color gradient from red to blue. Red indicates that the link is exiting the node (out-link), and blue indicates that the link is entering the node (in-link). Bilateral links are drawn in black. In this study, each rule could be classified to its corresponding Wolfram class more easily than in our previous study [8]. Networks of class II rules contain localized or thin and striped links. Class III rules have thick and complex networks. The network representation of additive rules, e.g., rule 90 and $T42$, is independent of an initial configuration, and it is equivalent to the rules and not merely a perturbed result. Consequently, the symmetric and geometric graphs in Tables 1 and 2 are all additive rules. Their geometric patterns drastically change depending on the time interval t_I. The networks of some class II rules and class IV candidates, rule 110 and $T11(T52)$, are sensitive to changes in an initial configuration. Such characteristics are represented by a large value of one of their clustering coefficient components, as described in the next section.

– Conway's Game of Life

The typical patterns of Life are known as still lifes, oscillators, and spaceships [14,15]. Although Block (Fig. 1a) and Beehive (Fig. 1b) are both typical still lifes, their networks show different behaviors to stop or continue their growth with t_I. Because the outermost in-links of Beehive indicate the spreading of the

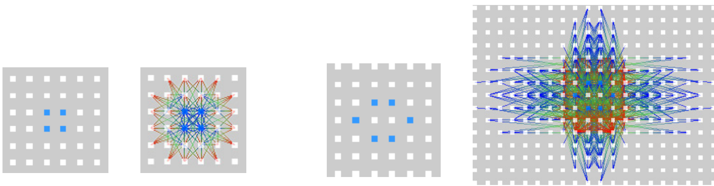

(a) Block

(b) Beehive at $t_I = 20$

Fig. 1. Typical Life patterns and their networks. Still lifes: (a) Block and (b) Beehive.

perturbations from the inner cells to the outer area, if a large value of t_I is considered, the blue edges may spread widely into the outer area. These edges represent the underlying tension in the Life rest state, leading to avalanches from one-cell perturbations (Fig. 2). Networks derived from other famous patterns such as Blinker and Glider can be found in our previous article [9] or a web site [16].

4 Network Parameters

Here, we use the efficiency [17,18] and the clustering coefficients (CCs) [19] to investigate the characteristics of the derived CA networks. The efficiency is the

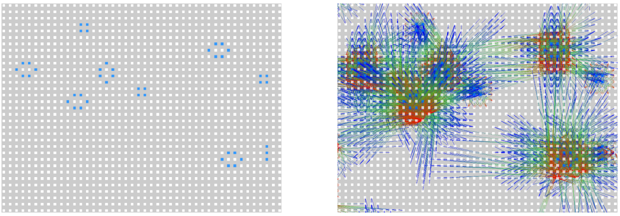

Fig. 2. Life in rest state and its network at $t_I = 25$

harmonic mean of the shortest path lengths from one node to the other nodes. The CCs of directed networks are divided into several types: cycle (C^{cyc}), middleman (C^{mid}), in (C^{in}), out (C^{out}), and the sum total of all the CCs (C^{all}) [20]. Graphs of the efficiency and C^{all} of the derived networks show a relation between network connectivity and Wolfram's classes. Radar charts of the efficiency and other CC components also illustrate characteristic figures reflecting the global and local connection properties of the derived networks. Typical class III rules, which can produce highly random bit sequences, have a pentagonal figure. The rules that are regarded as candidates for class IV occupy the area

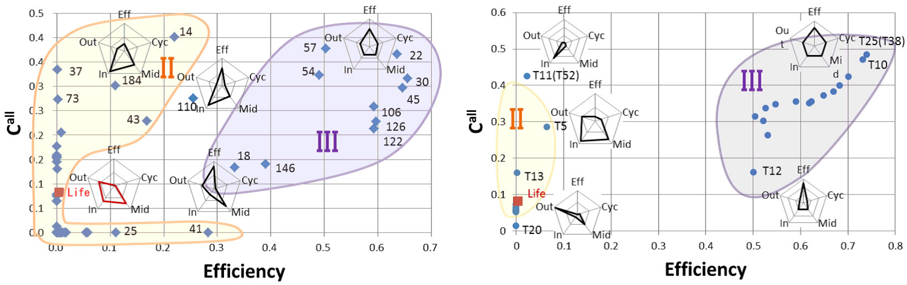

(a) ECA rules at $t_I = 1600$

(b) 5TCA rules at $t_I = 800$

Fig. 3. Efficiency/C^{all} graphs of networks derived from (a) ECA and (b) 5TCA rules, representing the average of networks obtained from ten pseudo-randomly generated initial configurations with $N = 3201$ and $t_0 = 10^4$. Efficiency/C^{all} value of Life network is also plotted with $N = 101 \times 101$, $t_0 = 10^5$, and $t_I = 50$. Radar charts show efficiency-CC components of networks derived from the typical rules, (a) 184, 110, 22, Life, and 18; and (b) T11(T52), T10, T5, T20 and T12 (from left top to right bottom). The five axes are (clockwise from the top) efficiency, C^{cyc}, C^{mid}, C^{in}, and C^{out}.

between class II and III rules (Fig. 3). Rule 184, which is known for its high-dependency on initial configurations [13], and similar class II rules, 14, 43 and $T5$, are represented by a large C^{in} relative to the other CC components [8]. The class IV candidates, rule 110 and $T11(T52)$, are also sensitive to changes in an initial configuration. The elimination of transients allows us to clearly observe the large value of C^{in} in their radar charts (Fig. 4). On the contrary, the large

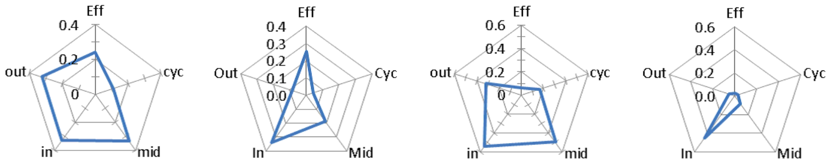

(a) Rule 110 (b) Rule $T11(T52)$

Fig. 4. Changes in radar charts of efficiency-CC components of class IV candidates, (a) rule 110 and (b) rule $T11(T52)$, with $N = 3201$. The left and right graphs in each figure are at $t_0 = 0$ and 10^4, respectively.

C^{in} figure of rule $T30$ changes to a pentagonal one which can be recognized as a class III characteristic (Fig. 5).

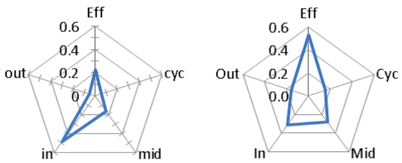

Fig. 5. Change in radar chart of efficiency-CC components of rule $T30$ with $N = 3201$. The left and right graphs are at $t_0 = 0$ and 10^4, respectively.

As reported in the previous paper [9], the Life rest-state network has a scale-free nature in its degree distribution. Seeking such a scale-free network in the ECA and 5TCA rules, we have found that a rule $T11(T52)$ network has scale-free-like degree distributions (Fig. 6). Although the power-law was not a plausible fit to the distributions according to a goodness-of-fit test [21], we checked the distributions of the lifetimes and sizes of the avalanches caused by one-cell perturbations of an attractor. The lifetime l can be defined by the number of time steps before the configuration returns to an attractor [11]. The size s is defined as the space-time sum of the changes in the out-degrees [12]:

$$s_i \equiv \sum_{t=1}^{l_i} |\, n^i_{out}(t) - n^i_{out}(t-1)\,|, \tag{5}$$

where l_i is the lifetime of the avalanche launched from the cell at i, and the out-degree of the cell is given by $n^i_{out}(t) = \sum_{j=0}^{N-1} [\boldsymbol{A}_R(t)]_{i,j}$. Fig. 7 shows the

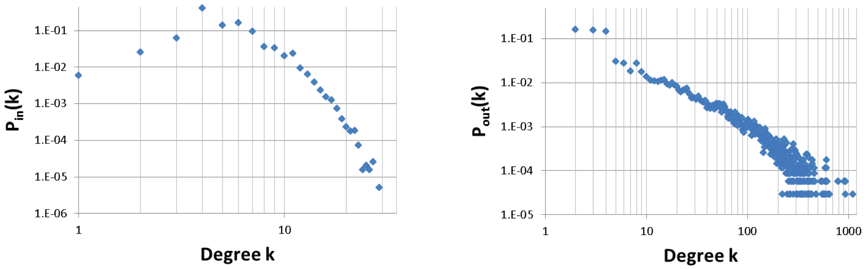

(a) In-degree distribution

(b) Out-degree distribution

Fig. 6. Log-log plots of normalized distributions of rule $T11(T52)$ representing the average of networks obtained from ten pseudo-randomly generated initial configurations with $N = 20001$, $t_0 = 2 \times 10^5$, and $t_I = 5000$.

power-law distributions of the lifetimes and sizes of avalanches. The statistical tests gave p-values larger than 0.1 at l_{min} and s_{min} larger than 200.

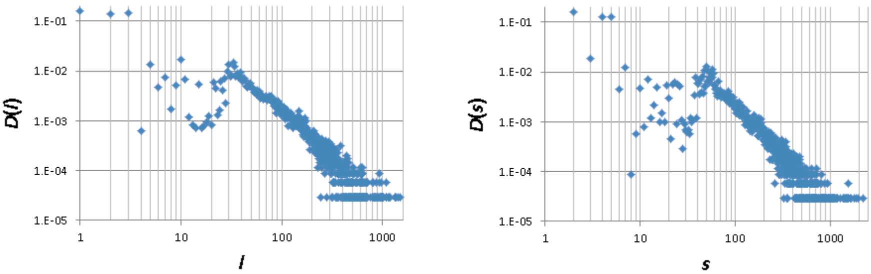

(a) Distribution of lifetimes

(b) Distribution of sizes

Fig. 7. Log-log plots of normalized distributions of the lifetimes and sizes of the avalanches of rule $T11(T52)$ representing the average of networks obtained from ten pseudo-randomly generated initial configurations with $N = 20001$, $t_0 = 2 \times 10^5$, and $t_I = 5000$.

5 Conclusions

Our network representation provides us with a new visualization scheme of binary CA rules. The networks derived from the independent ECA and 5TCA rules illustrate the symmetrical and dynamical features more clearly than in the previous study [8]; this is because of the removal of the transient effects of initial configurations. The network representation allows the techniques of the network theory to be used for the investigation of CA dynamics. The efficiency/CC graphs and the characteristic radar charts of the efficiency and the

CC components are useful for studying the global and local connection properties of derived networks. Similar to the Life rest-state network, the residual patterns of an attractor of class IV candidates may be connected to each other by the expansion of links, which creates the underlying tension that is the cause of avalanches, whose lifetimes and sizes show power-law distributions. In fact, the derived network of rule $T11(T52)$ has the power-law distributions of the lifetimes and sizes of the avalanches. Although Rule 110 is well-known as a class IV rule, thus far, we have not found such a scale-free nature in its distributions. If class IV behavior requires some fractal structures inside the system, a scale-free nature would be detected in its network representation. Further investigations will be required to clarify a relation between scale invariance and class IV behavior.

References

1. von Neumann, J.: The theory of self-reproducing automata. In: Burks, A.W. (ed.) Essays on Cellular Automata. University of Illinois Press (1966)
2. Wolfram, S.: Statistical mechanics of cellular automata. Rev. Mod. Phys. 55, 601–644 (1983)
3. Gardner, M.: Mathematical games. Scientific American 223, 120–123 (1970)
4. Berlekamp, E.R., Conway, J.H., Guy, R.K.: Winning Ways for Your Mathematical Plays, vol. 2. Academic Press, New York (1982)
5. Watts, D.J., Strogatz, S.H.: Collective dynamics of 'small-world' networks. Nature 393, 440–442 (1998)
6. Barabási, A.L., Albert, R.: Emergence of scaling in random networks. Science 286, 509–512 (1999)
7. Kayama, Y.: Complex networks derived from cellular automata. arXiv:1009.4509 (2010)
8. Kayama, Y.: Network representation of cellular automata. In: 2011 IEEE Symposium on Artificial Life (IEEE ALIFE 2011) at SSCI 2011, pp. 194–202 (2011)
9. Kayama, Y., Imamura, Y.: Network representation of the game of life. Journal of Artificial Intelligence and Soft Computing Research 1 (3), 233–240 (2011)
10. Bak, P., Tang, C., Wiesenfeld, K.: Self-organized criticality: an explanation of 1/f noise. Physical Review Letters 59 (4), 381–384 (1987)
11. Bak, P., Chen, K., Creutz, M.: Self-organized criticality in the 'game of life'. Nature (London) 342, 780 (1989)
12. Kayama, Y.: Network representation of the game of life and self-organized criticality (extended abstract). To be appeared in the Proceedings of the 13th International Conference on the Simulation & Synthesis of Living Systems (2012)
13. Wolfram, S.: A New Kind of Science. Wolfram Media, Inc. (2002)
14. Callahan, P.: Patterns, programs, and links for conway's game of life (1995), `http://www.radicaleye.com/lifepage/` (retrieved at February 1, 2011)
15. Flammenkamp, A.: Achim's game of life page (1998), `http://wwwhomes.uni-bielefeld.de/achim/gol.html` (retrieved at December 12, 2011)
16. Kayama, Y.: Network View of Conway's Game of Life. Wolfram Demonstrations Project (2012), `http://demonstrations.wolfram.com/NetworkViewOfConwaysGameOfLife/`
17. Latora, V., Marchiori, M.: Efficient behavior of small-world networks. Phys. Rev. Lett. 87, 198701–198704 (2001)

18. Boccaletti, S., Latora, V., Moreno, Y., Chavez, M., Hwang, D.U.: Complex networks: Structure and dynamics. Physics Reports 424, 175–308 (2006)
19. Wasserman, S., Faust, K.: Social Network Analysis. Cambridge University Press (1994)
20. Fagiolo, G.: Clustering in complex directed networks. Phys. Rev. E 76, 026107–026114 (2007)
21. Clauset, A., Shalizi, C.R., Newman, M.E.J.: Power-law distributions in empirical data. SIAM Review 51, 661–703 (2009)

Appendix: Sample Networks of ECA and 5TCA

All independent and non-trivial network graphs of ECA and 5TCA rules are shown in Table 2 and Table 1, respectively. The initial configurations of each of the 41 cells are pseudo-randomly generated, and their initial time t_0 is set to 1000.

Table 1. Independent networks of 5TCA rules obtained from pseudo-randomly generated initial configurations with $N = 41$, $t_0 = 1000$, and $t_I = 10$. The rules inside the square brackets are the diminished-radix complement to the one outside the brackets. It is hard to find a non-trivial network in rule $T20$ because of the small lattice size.

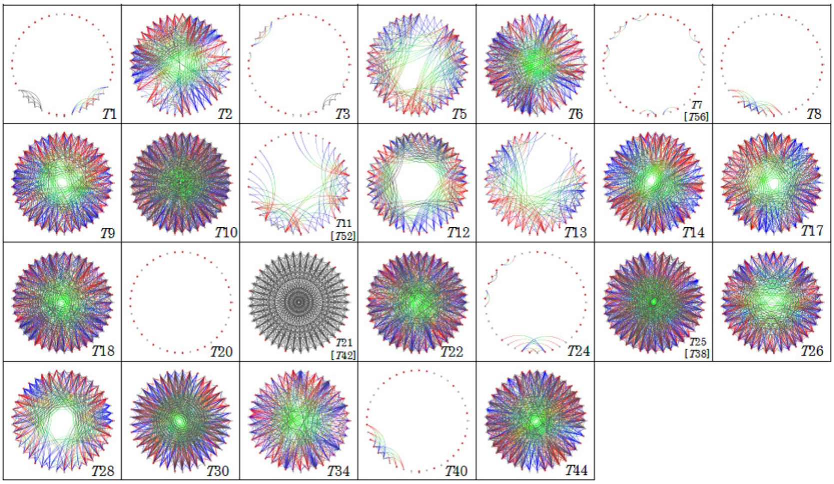

Table 2. Independent and non-trivial networks of ECA rules obtained from pseudo-randomly generated initial configurations with $N = 41$, $t_0 = 1000$, and $t_I = 20$. The rules inside the square brackets are the diminished-radix complement to the one outside the brackets.